Computers and Concrete, Vol. 11, No. 1 (2013) 63-73
DOI: http://dx.doi.org/10.12989/cac.2013.11.1.063

Experimental and numerical investigations of the influence of reducing cement by adding waste powder rubber on the impact behavior of concrete

Mustafa Maher Al-Tayeb[1], B.H. Abu Bakar*[1], Hazizan Md Akil[2] and Hanafi Ismail[2]

[1]*School of Civil Engineering, Universiti Sains Malaysia, Engineering Campus, 14300 Nibong Tebal, Penang, Malaysia*
[2]*School of Materials & Mineral Resources Engineering, Universiti Sains Malaysia, Engineering Campus, 14300 Nibong Tebal, Penang, Malaysia*

(Received December 10, 2011, Revised March 25, 2012, Accepted April 17, 2012)

Abstract. In this study, the effect of reducing cement by proportional addition of waste powder rubber on the performance of concrete under impact three-point bending loading were investigated experimentally and numerically. Concrete specimens were prepared by adding 5%, 10% and 20 % of rubber powder as filler to the mix and decreasing the same percentage of cement. For each case, three beams of 50 mm ×100 mm × 500mm were loaded to failure in a drop-weight impact machine by subjecting them to 20 N weight from 300mm height, while another three similar beams were tested under static load. The bending load-displacement behavior was analyzed for the plain and rubberized specimens, under static and impact loads. A three dimensional finite-element method simulation was also performed by using LUSAS V.14 in order to study the impact load-displacement behavior, and the predictions were validated with the experimental results. It was observed that, despite decreasing the cement content, the proportional addition of powder rubber until 10% could yield enhancements in impact tup, inertial load and bending load.

Keywords: rubber powder; cement concrete; compressive strength; impact energy; finite element method.

1. Introduction

Cement consumption is increasing day by day as the main constituent of concrete which is the most widely used construction material. Increased use of cement poses environmental challenge as 5% of the global anthropogenic CO_2 emission is originated from cement production (Humphreys and Mahasenan 2002).

Alongside this, there is increased generation of waste rubber which also has adverse ecological effects, due to its health hazards and difficulty for land filling. The high cost of disposal and requirement of large landfill area resulted in random and illegal dumping of waste rubber (Siddique and Naik 2004). As a promising solution to the aforementioned problems, the idea of adding waste crumb rubber to concrete as sand replacement has recently gained attraction, as it improves the flexibility and ductility of concrete (Son *et al*. 2011, Sukontasukkul and

*Corresponding author, Professor, E-mail: cebad@eng.usm.my

Chaikaew 2006). Substantial works were reported on the use of polymers such as tire rubber as a replacement for cement, sand or aggregates in concrete mixtures (Eldin and Senouci 1993, Ganjian *et al.* 2009, Li *et al.* 2004, Li *et al.* 1998, Son *et al.* 2011, Sukontasukkul and Chaikaew 2006, Taha *et al.* 2008, Terro *et al.* 2005, Topcu and Avcular 1997, Topcu 1995, Tortum *et al.* 2005), these studies revealed that the addition of rubber to concrete enhanced the elastic behavior, while reducing the compressive strength.

(Son *et al.* 2011) determined the strength, deformability and energy absorption capacity of reinforced concrete columns with waste tire rubber under static compression load. They found that using waste tire in concrete improved the energy absorption capacity and ductility. (Sukontasukkul and Chaikaew 2006) demonstrated that replacing coarse aggregate and sand with crumb rubber, enhanced the flexibility, toughness, energy absorption and ductility of concrete, with reduction in compressive and flexural strengths. During an impact test by 10 kg hammering from 60 mm height, (Taha *et al.* 2008) observed that the crump or chipped tire rubber particles in concrete could enhance the impact resistance. (Ganjian *et al.* 2009) studied the effect of partial replacement of cement by rubber powder and coarse aggregate by chipped rubber, on the flexural strength of concrete. They showed that the former process caused more reduction (37%) in flexural strength compared with the latter (29%).

In this study the effects of adding waste powder rubber by 5%, 10% and 20% with proportional decrease in cement content, on the impact load-displacement and fracture energy of concrete were investigated experimentally and the results were compared with those under static load and by FEM simulations. As far as the authors are aware, an analysis of this kind has not been reported so far. For each case, three beams of size 50 mm ×100 mm × 500mm were loaded to failure in a drop-weight impact machine which facilitated dropping 20 N weight from 300mm height, and similar specimens were tested under static load. The tup and bending load histories, and load-displacement behavior were analyzed for the plain and rubberized specimens. LUSAS V.14 software was employed for the simulations.

2. Materials and methods

2.1 Materials

The control mix was concrete with a compressive strength of 40MPa. The maximum coarse aggregate size was 20 mm, and the fine aggregate was natural sand, with specific gravities 2.64 and 2.66 respectively. Rubberized concrete specimens were named as Pr 5%, Pr 10% and Pr 20% corresponding to the additions of 5, 10 and 20% by volume of waste rubber powder (Fig.1) of particle size 0.15–0.6mm (Fig. 2) and relative density 0.6. The compositions of the plain and rubberized concrete samples are presented in Table 1.

For the compression and modulus of elasticity tests, three cylinders of height 200mm and diameter 100 mm were used for each type, according to ASTM C39/C39 M-01 and ASTM C 469-94. The specimens for three-point static and impact flexural loading tests were 100 mm wide, 50 mm deep and 400 mm long, with a loaded span of 300 mm. All specimens were cured in water for 28 days in accordance with ASTM C 192/C192M-06.

2.2 Experimental procedure

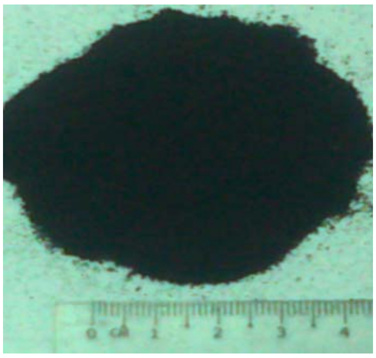

Fig. 1 Image of the rubber powder sample

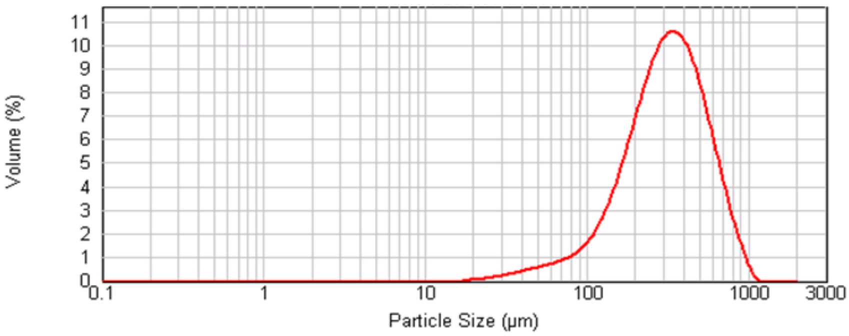

Fig. 2 Particle size distribution of rubber powder

Table 1 Mixture properties of plain and rubber powder concrete

Unit	Rubber percent	Cement	Water	Sand	Coarse aggregate	Crumb rubber
Weight (kg)	-	395	190	797	973	0
Volume (m^3)	0%	125	190	301	367	0
Weight (kg)	-	374	180	797	973	3.8
Volume (m^3)	5%	119	180	301	367	6.25
Weight (kg)	-	355	171	797	973	7.5
Volume (m^3)	10%	112	171	301	367	12.5
Weight (kg)	-	315	152	797	973	15
Volume (m^3)	20%	100	152	301	367	25

The three-point static flexural strength tests were performed according to ASTM C78–94.

Impact tests were conducted on an instrumented falling-weight impact machine as in Fig. 3; the machine facilitated dropping 2 kg hammer from variable heights of up to 2 m (drop height of 0.3m was chosen in this study). The impact load history during the test was measured using a Kistler933A piezo-electric load cell of 50 kN capacity. The specimens were supported by two steel cylinders of 10 mm diameter, positioned on movable right angled supports. The specimen

Fig. 3 The experimental impact flexural test rig

acceleration during impact was recorded by Dytran 3224A2 accelerometer with a range of ±2500g (g is gravitational acceleration) and Sensitivity 2 mV/g. Data from the load cell and the accelerometer were recorded at 0.2 ms intervals using a PC-based data acquisition system.

The tup load, P_t at the mid-span of the beam recorded by the load cell is the sum of inertial load (P_i) and bending load (Pb) acting at the center (Banthia 1987, Banthia *et al.* 1999, Banthia *et al.* 1987, Banthia *et al.* 1989). So

$$P_b = P_t - P_i \tag{1}$$

where *Pi* for linear distribution of accelerations along the beam is uniform.

$$Pi = \rho\, A\, a\, [L/3 + (8/3) \times (ov3/L2)] \tag{2}$$

where ρ: mass density of concrete; A: area of cross-section of the beam; a: acceleration at the center; L: span of the test beam and ov: length of the overhang.

The displacement histories at the load-point can be obtained by double integrating the acceleration history

$$d(t) = \int_0^t \int_0^t a(t)dt \tag{3}$$

The fracture energy was calculated as the area under impact bending load versus displacement curve (Banthia 1987, Banthia *et al.* 1999, Banthia *et al.* 1987, Banthia *et al.* 1989).

2.3 Finite element model

In order to simulate the behavior of rubberized concrete beams subjected to the impact load, LUSAS V.14 was used. The concrete beam was assumed to be built up with hexahedron elements

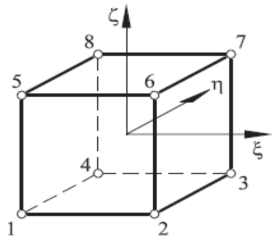

Fig. 4 The 8-node hexahedron and the natural coordinates ξ, η, ζ

(Fig. 4) whose corners have shape functions represented by Eq. (6) (Yang 1986).

$$N_i^{(e)}(\xi,\eta,\zeta)=\frac{1}{8}(1+\xi_i\xi)(1+\eta_i\eta)(1+\zeta_i\zeta) \tag{4}$$

The deformation was calculated by using the following expression

$$\{u\}=\sum_{i=1}^{np}[N_i]\{u_i\} \tag{5}$$

where $\{u\}$: the deformation vector at any location over the element; $\{u_i\}$: the deformation vector at the specified node of the element; $[N_i]$: the nodal shape function matrix of size (3 × 3) and np: the total number of the nodes in the element.

The boundary conditions (Fig. 5) were set as:

The tup load curve obtained from experiment was used to define the load at the location Pt (x=200 mm, y=50 mm, z=50 mm), and the beam was supported (uniformly distributed along z-direction) from bottom at locations, x =50 mm (support 1) and x =350 mm (support 2). To choose the appropriate mesh size, a number of trials were made and found that, after 1024 elements there was no improvement in accuracy; hence this mesh size was selected and the simulation took about 20 minutes, in a Pentium (R) dual-Core Processor: i5-3410M CPU @ 2.30 GHz 2.30 GHz; 4.00 GB RAM.

The nonlinear equilibrium equation (Chopra 1995, LUSAS 14) is given by

$$[M]\{a\}+[C]\{v\}+[K]\{d\}=\{f_e\} \tag{6}$$

where M is the mass matrix which is defined as

$$[M]=\sum_{e=1}^{n}\int_v [N]^{(e)T}[\rho]^{(e)}[N]^{(e)}\,dv \tag{7}$$

where N is the element shape function array and ρ is the density matrix. C is the Rayleigh damping matrix expressed by

$$[C]=a_R[M]+b_R[K] \tag{8}$$

where K is the structure stiffness matrix defined by

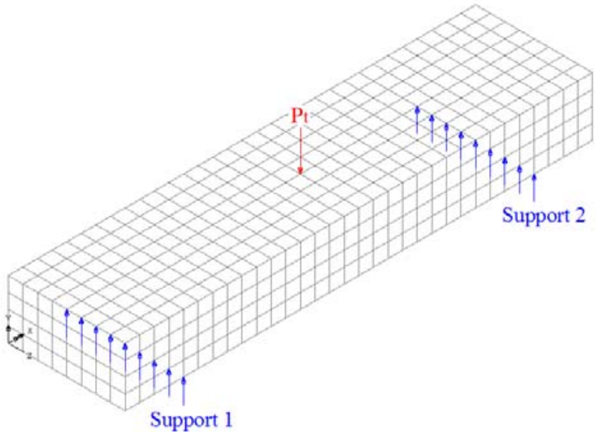

Fig. 5 Finite element model for the beam

$$[K]=\sum_{e=1}^{n}\int_{v}[B]^{(e)T}[D]^{(e)}[B]^{(e)}\,dv \qquad (9)$$

where B is the strain displacement matrix and D is material modulus matrix; a_R (Eq. (10)) and b_R (Eq. (11)) are the mass and stiffness respectively of Rayleigh damping coefficient.

$$a_R=\frac{2\varpi_f\varpi_s(\psi_s\varpi_f-\psi_f\varpi_s)}{(\varpi_f^2-\varpi_s^2)} \qquad (10)$$

$$b_R=\frac{2(\psi_f\varpi_f-\psi_s\varpi_s)}{(\varpi_f^2-\varpi_s^2)} \qquad (11)$$

where

ψ_f and ψ_s are the damping ratios of the structure for the first and second circular frequencies respectively.

Explicit scheme (central difference method) was used to determine the acceleration and thus the velocity and displacement increments for each time step. The central difference algorithm implemented in LUSAS 14 is as follows

For each time step n=1...N-1

$$Ma\ (t_n)=f\ (t_n) \qquad (12)$$

$$v(t_{n+1/2})=v(t_{n-1/2})+\frac{1}{2}a(t_n)[\,\Delta t_n-\Delta t_{n-1}] \qquad (13)$$

$$d\ (TN+_1)=d\ (t_n)+v\ (t_{n+1/2})\ \Delta tn \qquad (14)$$

where a, v and d are the acceleration, velocity and displacement of any node.

3. Results and discussion

3.1 Experimental results

The results of compressive stress and modulus of elasticity are given in Table 2. It is observed that, the average compressive stress of the plain concrete in 28 days is 37MPa. As the cement volume is decreased with proportional addition of rubber powder, the compressive stress reduces by 19, 32 and 51% with 5, 10 and 20 % of volumes respectively. The elastic modulus was also found to decrease by 10, 17 and 28% respectively compared with the plain concrete. Similar observations were also reported by (Ganjian *et al.* 2009).

The variation of tup load with time is shown in Fig. 6 which illustrates that the total impact load increases with the addition of 5% and 10% of rubber powder and proportional reduction of cement volume. Although the peak tup load for Pr 20% is less than that for Pr 10%, it is still higher than that of the plain concrete. The enhanced total impact load is attributed to the high plastic energy capacity of rubber compared to the normal concrete (Topcu 1995); hence, addition of rubber improves the ductility and impact absorption capacity of the mix.

Table 2 Compressive strength and modulus of elasticity

Concrete type	Average compressive stress (MPa)	Average elastic modulus (kN/mm^2)
Plain	37	29
Pr 5%	30	26
Pr 10%	25	24
Pr 20%	18	21

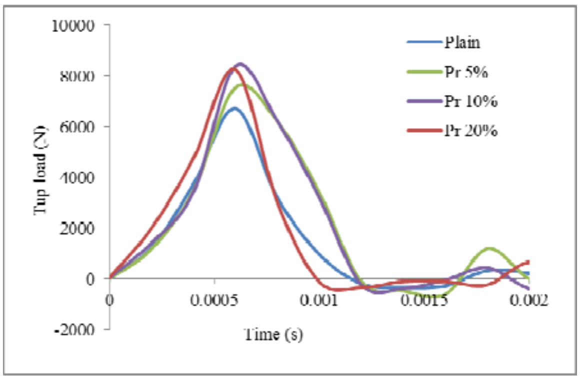

Fig. 6 Tup load history

Figs. 7(a)-(d) shows the variations in tup, inertial and bending loads with time, for plain and rubberized concretes. The inertial load was calculated from Eq. (2) and the bending load was obtained by subtracting inertial load from tup load. It is observed that both the inertial and bending loads increase for Pr 5% and Pr 10%, and then decrease slightly for Pr 20% but still higher than those of plain concrete. The enhanced inertial load is due to the increase in flexibility of the mix by adding rubber. The increase of bending load of the rubberized concrete is attributed to the high plastic energy capacities of rubber (Topcu 1995); adding rubber improves the ductility and ability to absorb impact energy. It was established that, the replacement of coarse aggregate by rubber caused increase in impact energy (Taha *et al.* 2008, Topcu and Avcular 1997).

Fig. 8 shows the calculated impact bending load against deflection plots for the plain concrete, Pr 5%, Pr 10% and Pr 20%. Table 4 summarizes the fracture energies for the plain and rubberized concrete specimens. The dynamic fracture energy is higher than the static fracture energy as also observed in the previous works (Banthia 1987, Banthia *et al.* 1999, Banthia *et al.* 1987, Banthia *et al.* 1989, Jerome and Ross 1997) where plain concrete was used as control mix. The fracture energy of the plain concrete under impact load is 1.17 Nm. For Pr 5% and Pr 10%, the fracture energy increases by 50% and 65% respectively, while there is only 6% increase for Pr 20%.

3.2 Comparison of dynamic and static test results

Table 3 shows the comparison between the results obtained from static bending and impact bending tests. Generally the static peak bending load is less than the impact peak bending load; this is consistent with the published works (Banthia 1987, Banthia *et al.* 1999, Banthia *et al.* 1987, Banthia *et al.* 1989, Jerome and Ross 1997). It is also observed that that the ratio between dynamic and static peak bending loads increases with increase in the percentage of rubber powder. This is because adding rubber to concrete with proportional decrease in cement content decreases its

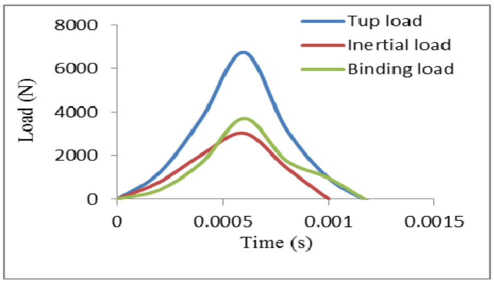

Fig. 7a Plain concrete

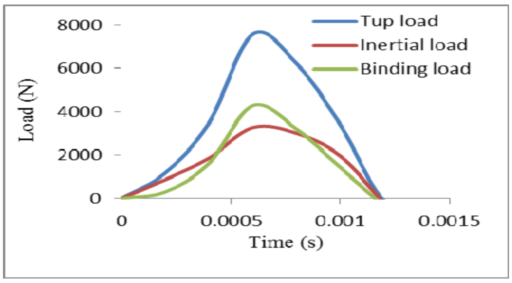

Fig. 7b Pr 5%

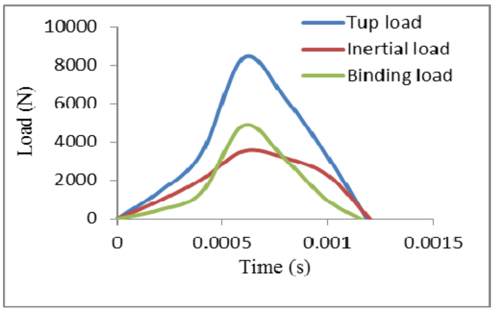

Fig. 7c Pr 10%

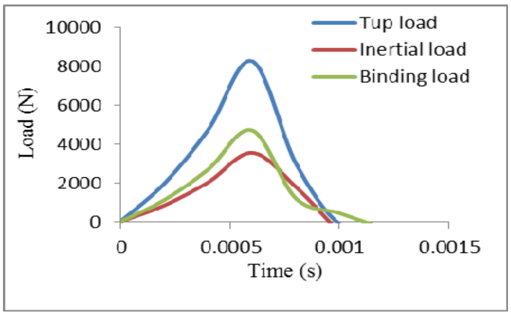

Fig. 7d Pr 20%

Fig. 7 Variations in tup, inertial and binding loads with time

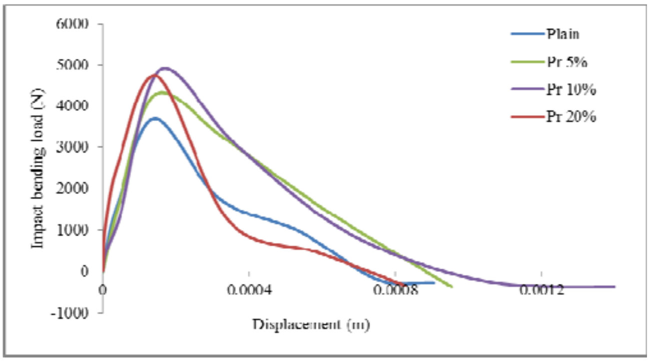

Fig. 8 Impact bending load against deflection

Table 3 Comparison of experimental static and impact bending

Concrete mixes	Static test		Impact test		Dynamic/Static	
	Peak bending load (N)	Fracture energy (N.m)	Peak bending load (N)	Fracture energy (N.m)	Peak bending load	Fracture energy
Plain	3417	0.408	3701	1.17	1.08	2.87
Pr 5%	2953	0.428	4282	1.79	1.45	4.18
Pr 10%	2507	0.458	4863	1.94	1.94	4.24
Pr 20%	2269	0.422	4705	1.24	2.07	2.94

strength under static load, but the ability of rubber to absorb dynamic energy enhances the strength of concrete under impact load. However the ratio between dynamic and static fracture energy increases for Pr 5% and Pr 10% only, and for Pr 20% it decreases but still more than that of the plain concrete.

3.3 Comparison of simulation and experimental results

3.3.1 Comparison of simulation and experimental results

The predicted impact load vs. displacement behaviors for plain concrete and three types of rubberized concretes were compared with the respective experimental results, as illustrated in Fig. 9 which demonstrate the strength of the proposed model in handling the problem. Compared to the plain concrete, the rubberized concrete samples show some discrepancies which are acceptable. For the plain concrete the displacement at the end of impact response is 1 mm in simulation, and 0.8 mm in experiment. As the rubber is added, the respective magnitudes of displacement increase slightly for 5% and 10% rubber additions; this is attributed to the high ductility of rubber compared to the normal concrete (Topcu 1995). However, for rubber additions of 20%, the displacement magnitudes decrease; this is due to the lack of proper bonding between concrete ingredients, which causes cracks at the boundary between aggregate and cement (Ganjian *et al.* 2009). This observation correlates well with the bending load vs. displacement behavior in Fig. 8.

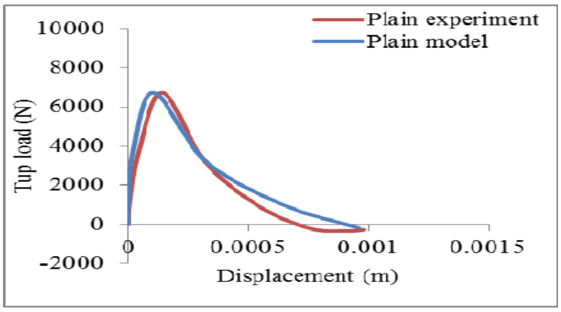

Fig. 9a Plain concrete

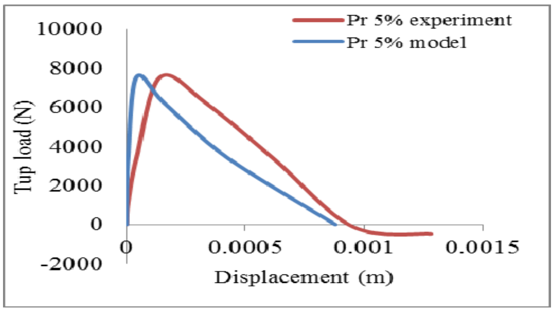

Fig. 9b Pr 5%

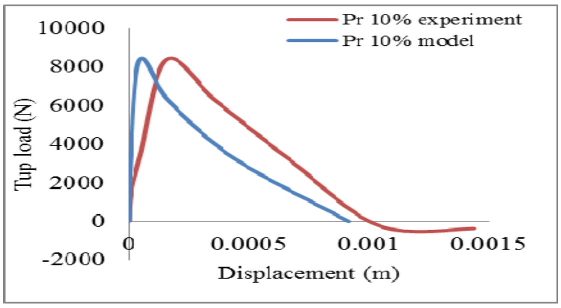

Fig. 9c Pr 10%

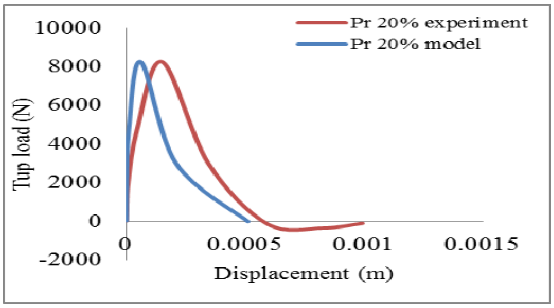

Fig. 9d Pr 20%

Fig. 9 Comparison of experimental and model results on impact load against displacement

4. Conclusions

The experimental observations of impact load-displacement behavior were well matched with the numerical predictions obtained by the proposed FEM model. It was worth noting that, the reduction in cement volume by adding rubber powder obtained improved the impact tup, inertial load and bending load up to 10%; at 20%, although a slight decrease was noticed, the results were still better than those of plain concrete. The static peak bending load was always decreasing with the decrease of cement volume, and the impact bending energies were always larger than the static energies. The proposed modeling approach would be a promising contribution to facilitate realistic predictions of rubberized concretes, thereby eliminating the tedious and risky experimental procedures.

References

Banthia, N. (1987), *Impact resistance of concrete*, University of British Columbia.

Banthia, N., Gupta, P. and Yan, C. (1999), "Impact resistance of fiber reinforced wet-mix shotcrete part 1: Beam tests", *Mater. Struct.*, **32**(8), 563-570.

Banthia, N., Mindess, S. and Bentur, A. (1987), "Impact behaviour of concrete beams", *Mater. Struct.*, **20**(4), 293-302.

Banthia, N., Mindess, S., Bentur, A. and Pigeon, M. (1989), "Impact testing of concrete using a drop-weight impact machine", *Exp. Mech.*, **29**(1), 63-69.

Chopra, A.K. (1995), *Dynamics of structures: theory and applications to earthquake engineering*, Prentice Hall Englewood Cliffs, New Jersey.
Eldin, N.N. and Senouci, A.B. (1993), "Rubber-tire particles as concrete aggregate", *J. Mater. Civil. Eng.*, **5**(4), 478-496.
Ganjian, E., Khorami, M. and Maghsoudi, A.A. (2009), "Scrap-tyre-rubber replacement for aggregate and filler in concrete", *Constr. Build. Mater.*, **23**(5), 1828-1836.
Humphreys, K. and Mahasenan, M. (2002), "Toward a sustainable cement industry", *Substudy 8: Climate Change*.
Jerome, D. and Ross, C. (1997), "Simulation of the dynamic response of concrete beams externally reinforced with carbon-fiber reinforced plastic", *Comput. Struct.*, **64**(5-6), 1129-1153.
Li, G., Stubblefield, M.A., Garrick, G., Eggers, J., Abadie, C. and Huang, B. (2004), "Development of waste tire modified concrete", *Cement. Concrete. Res.*, **34**(12), 2283-2289.
Li, Z., Li, F. and Li, J. (1998), "Properties of concrete incorporating rubber tyre particles", *Mag. Concrete. Res.*, **50**(4), 297-304.
Siddique, R. and Naik, T.R. (2004), "Properties of concrete containing scrap-tire rubber-an overview", *Waste. Manage.*, **24**(6), 563-569.
Son, K.S., Hajirasouliha, I. and Pilakoutas, K. (2011), "Strength and deformability of waste tyre rubber-filled reinforced concrete columns", *Constr. Build. Mater.*, **25**(1), 218-226.
Sukontasukkul, P. and Chaikaew, C. (2006), "Properties of concrete pedestrian block mixed with crumb rubber", *Constr. Build. Mater.*, **20**(7), 450-457.
Taha, M.M.R., El-Dieb, A., El-Wahab, M.A.A. and Abdel-Hameed, M. (2008), "Mechanical, fracture, and microstructural investigations of rubber concrete", *J. Mater. Civil Eng.*, **20**(10), 640-649.
Terro, M.J., El-Hawary, M.M. and Hamoush, S.A. (2005), "Inelastic analysis of concrete beams strengthened with various fiber reinforced polymer (FRP) systems", *Comput. Concrete*, **2**(3), 177-188.
Topcu, I. and Avcular, N. (1997), "Collision behaviours of rubberized concrete", *Cement Concrete Res.*, **27**(12), 1893-1898.
Topcu, I.B. (1995), "The properties of rubberized concretes", *Cement. Concrete. Res.*, **25**(2), 304-310.
Tortum, A., Çelik, C. and Cüneyt Aydin, A. (2005), "Determination of the optimum conditions for tire rubber in asphalt concrete", *Build. Environ.*, **40**(11), 1492-1504.
Yang, T. (1986), *Finite element structural analysis*, Prentice-Hall.

CC